

Received: 2015.07.07
Accepted: 2015.08.21
Published: 2015.09.14

A Biocompatible Reconstituted High-Density Lipoprotein Nano-System as a Probe for Lung Cancer Detection

Authors' Contribution:
Study Design A
Data Collection B
Statistical Analysis C
Data Interpretation D
Manuscript Preparation E
Literature Search F
Funds Collection G

A 1 **Hongxiu Lu**
D 1 **Hongguang Zhang**
C 2 **Dong Zhang**
F 3 **Hongwang Lu**
A 4 **Dedong Ma**

1 Department of Anaesthesiology, Affiliated Hospital of Shandong University of Traditional Chinese Medicine, Jinan, Shandong, P.R. China
2 Department of Stomatology, Qilu Hospital, Shandong University, Jinan, Shandong, P.R. China
3 Department of Stomatology, College of Physics, Shandong University, Jinan, Shandong, P.R. China
4 Department of Pulmonary Medicine, Qilu Hospital, Shandong University, Jinan, Shandong, P.R. China

Corresponding Author: Dedong Ma, e-mail: mddedong@163.com

Source of support: Financial supports from the National Natural Science Foundation of China (No. 81001043 and 81372333), the China Postdoctoral Science Foundation (No. 2012T50583), the Doctor Foundation of Shangdong Province (No. BS2010YY025), the Fundamental research fund of Shandong University (No. 2014YQ001), and the Science and Technology Planning Project of Shangdong Province (No. 2012GGE27097)

Background: Early detection of cancer is critical and is expected to contribute significantly to the success of cancer therapy and improvement of patient survival rates.





Material/Methods: A biocompatible, reconstituted, high-density lipoprotein (rHDL)-based nano-system containing calcium carbonate and near-infrared fluorescence dye (NIRF), methylene blue (MB), was fabricated and characterized by particle size, zeta potential, and morphology observation. The safety profile was confirmed by bovine serum albumin (BSA) challenge assay, hemolysis test, MTT assay, and *in vivo* long-term toxicity assay. The tumor targetability was assessed by cellular uptake, competitive inhibition experiments, and *in vivo* imaging assay.

Results: The self-assembled rHDL/MB/CCPs exhibited desirable and homogenous particle size, neutral surface charges, high bovine serum albumin stability, low hemolytic activity, and negligible cytotoxicity *in vitro*. The results obtained from confocal scanning laser microscopy and flow cytometry indicated that SR-BI coating exerted tumor-targeting function, which induced high and specific cellular uptake of rHDL/MB/CCPs. *In vivo* investigation in an A549 tumor xenografts-bearing mouse model revealed that rHDL/MB/CCPs possessed strong tumor targetability.

Conclusions: rHDL/MB/CCPs could be a safe tumor-targeting probe for cancer detection.

MeSH Keywords: **Early Detection of Cancer • High-Density Lipoproteins, Pre-beta • Lung Neoplasms**

Full-text PDF: <http://www.medscimonit.com/abstract/index/idArt/895255>

 2377  —  6  14



Background

Early detection of cancer is critical and is expected to contribute significantly to the success of cancer therapy and improvement of patient survival rates [1]. Fluorescence imaging, an optical imaging approach, is a desirable modality for early detection of cancer because of its high sensitivity and multiplex detection abilities, which essentially depends on the probes emitting in the near-infrared fluorescence (NIRF) spectrum window (650–900 nm wavelengths) [2]. Nanoparticle-based NIRF probes have overcome some of the limitations of the conventional NIRF organic dyes, such as insufficient stability in biological systems and low detection sensitivity. Therefore, a much effort has been made to actively develop novel NIRF nanoparticles for *in vivo* cancer molecular imaging [3]. Methylene blue (MB) is well recognized as one of the most inexpensive kinds of commercially available NIRF probes. Its application in bioanalysis has been widely explored [4]. However, its application in cancer detection is limited due to its lack of reactive functional groups and its high hydrophilicity, which makes it difficult to conjugate or effectively incorporate into conventional nanoparticles such as micelles and liposomes.

Calcium carbonate nanoparticles (CCPs) are emerged as a promising vector to deliver drugs and genes by means of physical adsorption and/or chemical embedment [5]. The well-formed CCPs with nano-scaled diameter exhibit low cytotoxicity and high biocompatibility both *in vitro* and *in vivo* [6]. To use CCPs in cancer detection, targeting ligands should be properly introduced. Apolipoprotein A-I (apoA-I) is the major protein component (~70%) in the natural high-density lipoprotein (HDL) of the lipid transport system and has been proved to have high affinity to the scavenger receptor-BI (SR-BI), which is primarily expressed on most malignant cells [7]. Endogenous HDL has non-immunogenicity and complete biodegradation. Reconstituted HDL (rHDL) is generally recognized as the synthetic form of endogenous HDL, and they possess similar physical and chemical properties. It has been well-documented that rHDL is a preferable carrier with promising application potential *in vivo* [7,8].

In the present study, we used a reverse water-in-oil micro-emulsion to entrap MB by calcium carbonate precipitate in a nano-sized reactor. The obtained MB-doped CCPs (MB-CCPs) were further modified using amphiphilic phospholipid dioleoylphosphatidic acid (DOPA) and then used to assemble a liposome (Lipos/MB-CCPs) together with dioleoylphosphatidylcholine (DOPC) and cholesterol. Finally, apoA-I was coated on the surface of Lipos/MB-CCPs to construct rHDL/MB-CCPs. It is expected that the rHDL/MB-CCPs may serve as a biocompatible probe to selectively detect lung cancer.

Material and Methods

Cell culture and animal model

A549 cell line, a gift from the Cell Bank of the Chinese Academy of Sciences (Shanghai, China), was cultured in DMEM medium (Gibco, USA) containing 10% FBS (HyClone, USA), 100 U/ml penicillin, and 100 µg/ml streptomycin (Gibco, USA) in a humidified atmosphere of 95% air/5% CO₂ incubator at 37°C.

Male BALB/c nude mice, age 5 weeks and weight 20–22 g, were purchased from the Shanghai Laboratory Animal Center (SLAC, China) and housed in the SPF II lab with free access to sterilized food and water. All procedures were carried out in strict compliance with NIH and our institutional guidelines for care and use of research animals. The tumor-bearing mouse model was established by subcutaneously inoculating suspension of A549 cells (1×10⁶ cells in 0.1 ml physiological saline) into the flanks of mice.

Preparation of rHDL/MB-CCPs

The procedure for the synthesis of Lipos/MB-CCPs followed that of a previously reported method, with some modifications [9]. We dispersed 300 µl of 100 mM CaCl₂ with 100 µl of 10 mg/ml MB in 11 ml cyclohexane/Triton X-100/n-hexenol (77/18/16 V/V) solution to form a very well-dispersed water-in-oil reverse micro-emulsion. The carbonate part was prepared by 300 µl of 100 mM NH₄CO₃ in a separate 2-ml oil phase. Two hundred µl (20 mg/ml) DOPA in chloroform was added to the carbonate phase. After mixing the above 2 solutions for 20 min, 30 ml of absolute ethanol was added to the micro-emulsion and the mixture was centrifuged at 12 000 g for at least 15 min to remove organic solvent and surfactant. After being extensively washed by ethanol 2–3 times, the MB-CCPs were dissolved in 1 ml of chloroform. The MB-CCPs solution was mixed with 100 µl of 10 mM DOPC/cholesterol (1:1). After evaporating the chloroform, the residual lipid was dispersed in 400 µl of 5 mM Tris-HCl buffer (pH=7.4) and incubated with 100 µl of apoA-I solution (30 mg/ml in PBS buffer) to formulate rHDL/MB-CCPs using proper stirring speed at 25°C for 8 h.

Particle size, zeta potential, and morphology of rHDL/MB-CCPs

Particle size and zeta potential of rHDL/MB-CCPs were measured at 37°C by dynamic light scattering (DLS) and electron light scattering (ELS), respectively, with a Malvern Zetasizer (Nano ZS-90, Malvern instruments, UK). The morphology was further observed by transmission electron microscope system (Hitachi, Japan) under the accelerating voltage of 80 kV.

Biocompatibility assays

Bovine serum albumin (BSA) challenging assay

rHDL/MB-CCPs were incubated with various BSA solutions (pH 7.4) for 1 h in a water bath (37°C). The alteration in turbidity (350 nm) was recorded with a spectrophotometer (Hitachi, Japan) [10].

Hemolysis test

For hemolysis testing, fresh rabbit red blood cells (RBCs) were collected and suspended in 0.1 M of sodium phosphate buffer to prepare a 2% (v/v) RBCs suspension. The rHDL/MB-CCPs with different concentrations were incubated with RBCs for 1 h in a 37°C water bath, centrifuged at 3000 rpm for 10 min, and the supernatants were measured at 540 nm by spectrophotometry. Positive (100% hemolysis) and negative controls (0% hemolysis) were obtained by mixing RBCs suspension with water or sodium phosphate buffer.

Cytotoxicity assay

The cytotoxicity of rHDL/MB-CCPs was evaluated using the standard MTT assay. Human pulmonary carcinoma A549 cells were seeded at 1.0×10^4 cells per well into 96-well plates with continuous culturing in DMEM medium (with 10% fetal bovine serum, incubated at 37°C and 5% CO₂ environment) overnight until 70–80% cell confluence. The primary growth medium was replaced with another 200 µl of fresh serum-free DMEM medium, in which rHDL/MB-CCPs were calculated to maintain in the range of 10–1000 µg/ml. The plates were further incubated for another 24 h, following with the addition of 20 µl of MTT solution (5 mg/ml in PBS) to each well. After that, the plates were returned to the incubator. Four hours later, the medium in each well was carefully replaced by 150 µl of DMSO and measured at 570 nm by use of a Microplate Reader (EL800, BIO-TEK Instruments Inc., USA). Untreated cells were taken as a control with 100% viability.

In vivo long-term toxicity

Ordinary BALB/c nude mice were randomly divided into 2 groups: 1) saline as control; 2) rHDL/MB-CCPs. Both formulations were administrated once every day for 14 days. After the administration, mice were skilled and the main organs were subjected to hematoxylin-eosin (HE) staining and observed under an optical microscope (OlympusIX51, Japan).

In vitro cellular uptake and competitive inhibition experiments

A549 cells were cultured on 6-well plates as mentioned above. Lipos/MB-CCPs and rHDL/MB-CCPs were co-incubated with the

cells for various time intervals. To further determine the SR-BI receptor-mediated internalization of rHDL/MB-CCPs, A549 cells were pretreated with excess apoA-I before the addition of rHDL/MB-CCPs. The fluorescence images were visualized and captured by confocal scanning laser microscopy (CSLM, Leica TCS SP5, Germany). At the same time, the fluorescence intensity of different groups was also quantitatively assessed by a flow cytometry (Becton Dickinson, USA).

In vivo tumor imaging

A549 tumor-bearing nude mice with tumor volume of approximately 100 mm³ (calculated according to the formula: $(L \times S^2)/2$, where L and S are the longest and shortest diameter, respectively) were intravenously administered with Lipos/MB-CCPs and rHDL/MB-CCPs. The images of nanoparticle biodistribution at different time points were recorded using the *In Vivo* Imaging System (FXPRO, Kodak, USA, NIR filter sets: excitation/emission, 680/790 nm) to evaluate their tumor targetability.

Results

Particle size, zeta potential, and morphology of rHDL/MB-CCPs

As displayed in Figure 1, rHDL/MB-CCPs showed nanoscale size of approximately 80 nm with neutral surface charges. The images obtained by TEM further demonstrated that rHDL/MB-CCPs were compacted and spherical nanoparticles with good dispersion. The particle size and zeta potential of Lipos/MB-CCPs were also investigated, revealing that Lipos/MB-CCPs has a smaller particle size (65 nm) and a negative surface charge of –20 mV (data not shown).

Biocompatibility assays

As depicted in Figure 2A, rHDL/MB-CCPs exhibited low absorption value with negligible turbidity change with the increase of BSA concentrations, as evidenced by the invariant OD_{350nm}.

Figure 2A shows that rHDL/MB-CCPs did not display significant hemolytic activity at any tested concentrations (<3%). The results obtained from cytotoxicity assay in Figure 2B demonstrated that A549 cells treated with various concentrations of rHDL/MB-CCPs, even at the highest concentration of 1000 µg/ml, achieved an almost identical viability as the control group (untreated cells). In the long-term toxicity assay, after 14 days of continuous injection of rHDL/MB-CCPs, the main organs of mice were excised for HE staining. As displayed in Figure 3, compared to the saline group, all the organs from rHDL/MB-CCPs mice were normal and healthy, with no pathological changes.

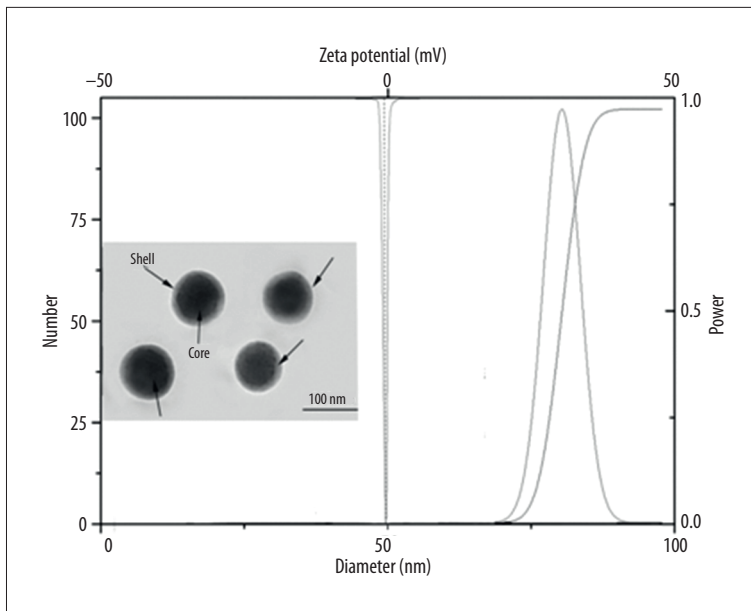


Figure 1. Particle size, zeta potential, and morphology of rHDL/MB-CCPs. Scale bar: 100 μm .

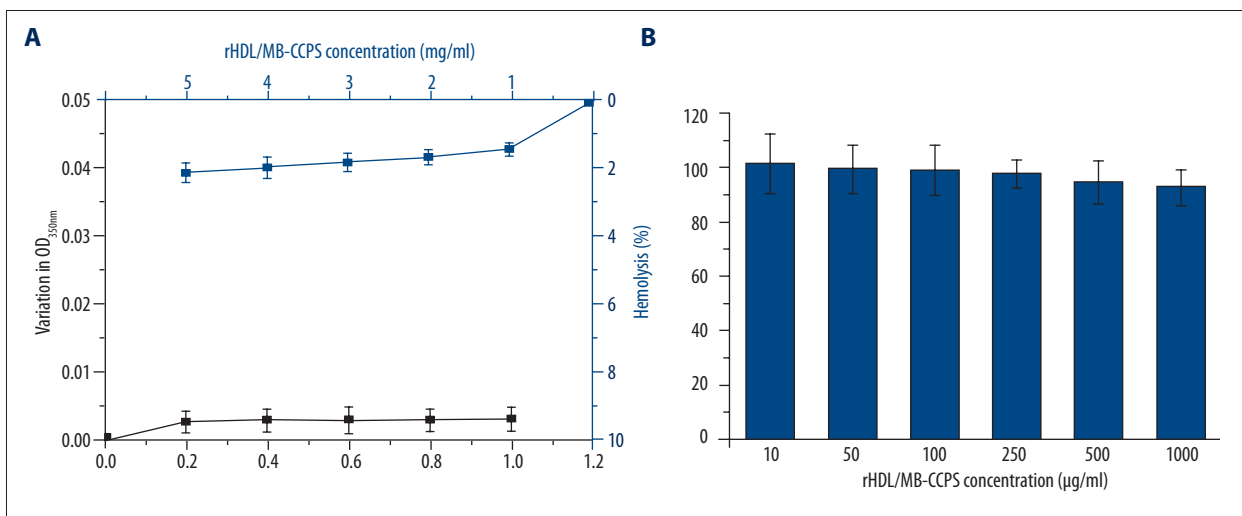


Figure 2. (A) BSA challenging assay and hemolysis test, (B) cytotoxicity assay of rHDL/MB-CCPs. Data are expressed as mean \pm S.D. (n=5).

***In vitro* cellular uptake and competitive inhibition experiments**

As shown in Figure 4, CSLM observations at 2 and 4 h revealed red fluorescence signals in the cytoplasm of A549 cells. In addition, the fluorescence signal gradually became stronger with extended incubation time. However, under the same conditions, rHDL/MB-CCPs displayed remarkably higher intensity compared with Lipos/MB-CCPs. The fluorescence intensity of rHDL/MB-CCPs was approximately 6.83-fold higher than that of Lipos/MB-CCPs after incubation for 4 h (Figure 4B). A competitive experiment was performed by treating A549 cells with free apoA-I prior to incubation with the nanoparticles. Fluorescence microscopy and flow cytometry demonstrated a

decrease in the fluorescence intensity in tumor cells pretreated with apoA-I compared with the untreated cells (Figure 4C, 4D).

***In vivo* tumor imaging**

As displayed in Figure 5, compared with Lipos/MB-CCPs, at 2 h after injection, rHDL/MB-CCPs were rapidly accumulated at the tumor site. Moreover, higher accumulation and retention of rHDL/MB-CCPs within the tumor region were detected at 4 h after injection. At 6 h, the rHDL/MB-CCPs were clearly retained in the tumor site with further increased fluorescence intensity, while the fluorescence intensity in Lipos/MB-CCPs group was only as strong as that of rHDL/MB-CCPs at 2 h.

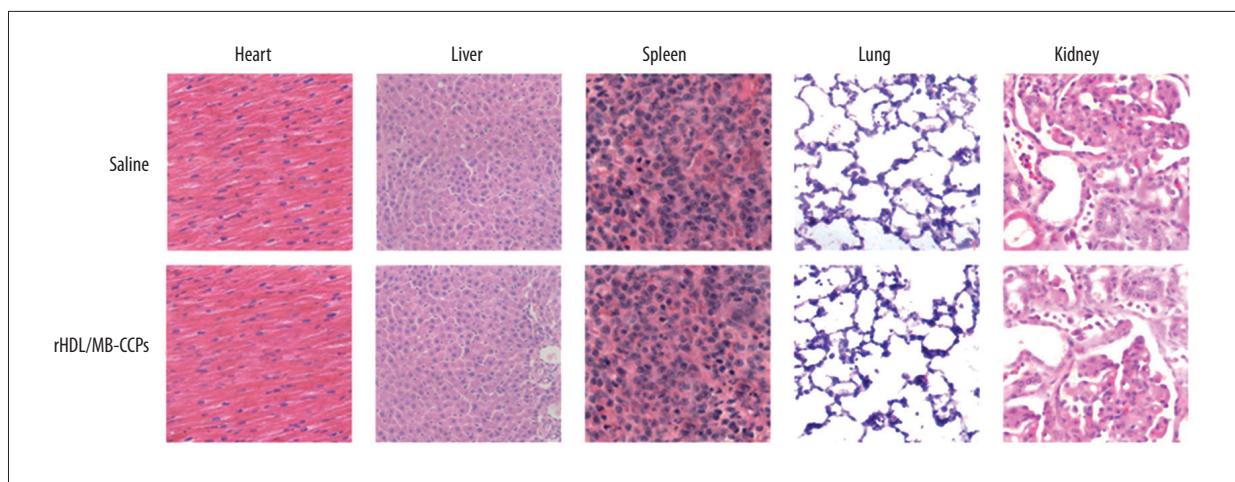


Figure 3. HE staining images (200×) of main organs from mice receiving saline and rHDL/MB-CCPs, respectively.

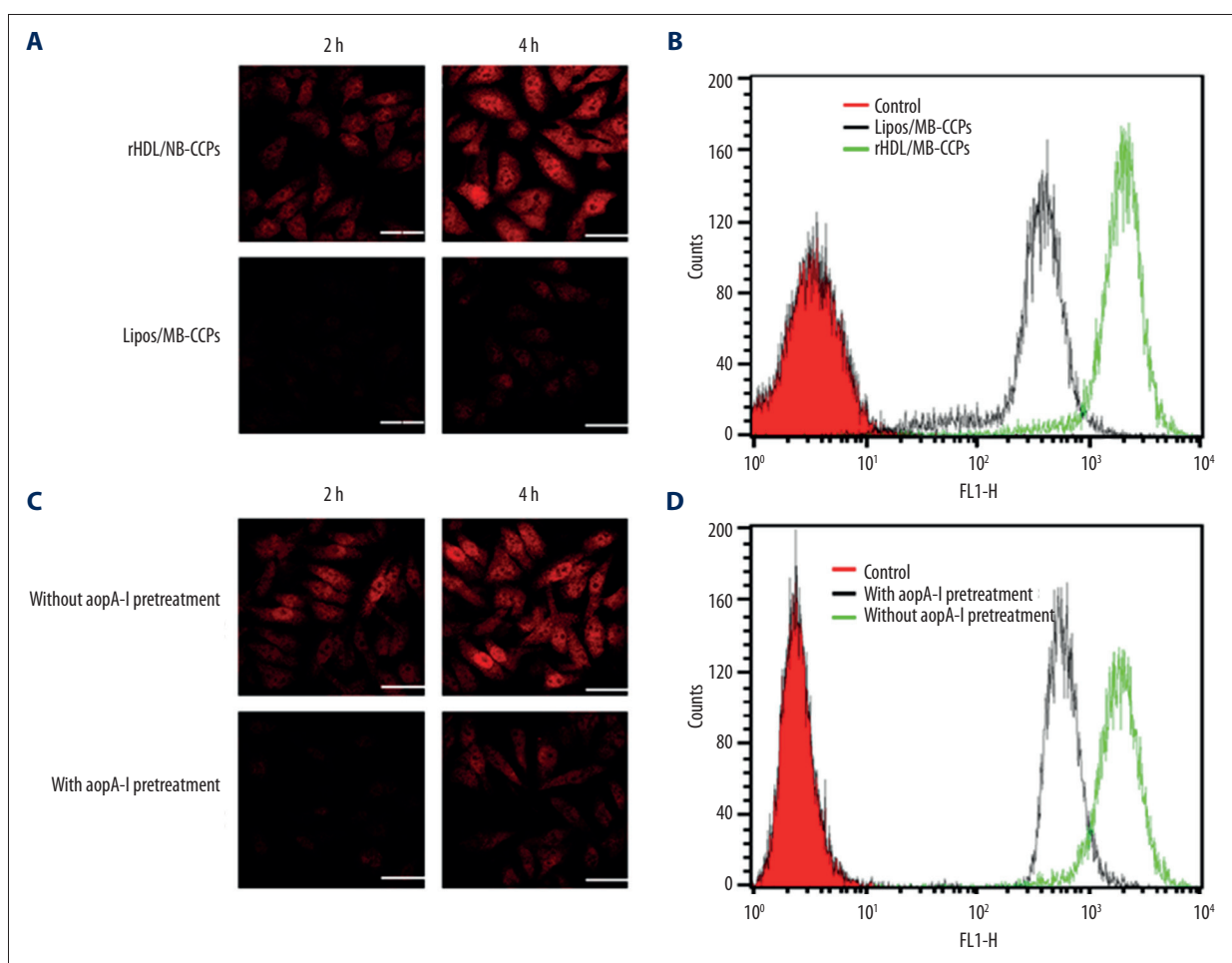


Figure 4. (A) CSLM images of cellular uptake profile of Lipos/MB-CCPs and rHDL/MB-CCPs at 2 h and 4 h after incubation. (B) Representative flow cytometry analysis of Lipos/MB-CCPs and rHDL/MB-CCPs at 4 h after incubation. (C) CSLM images of cellular uptake profile of rHDL/MB-CCPs pretreated with or without apoA-I at 2 h and 4 h after incubation. (D) Representative flow cytometry analysis of rHDL/MB-CCPs pretreated with or without apoA-I at 4 h after incubation. Scale bar: 25 μ m.

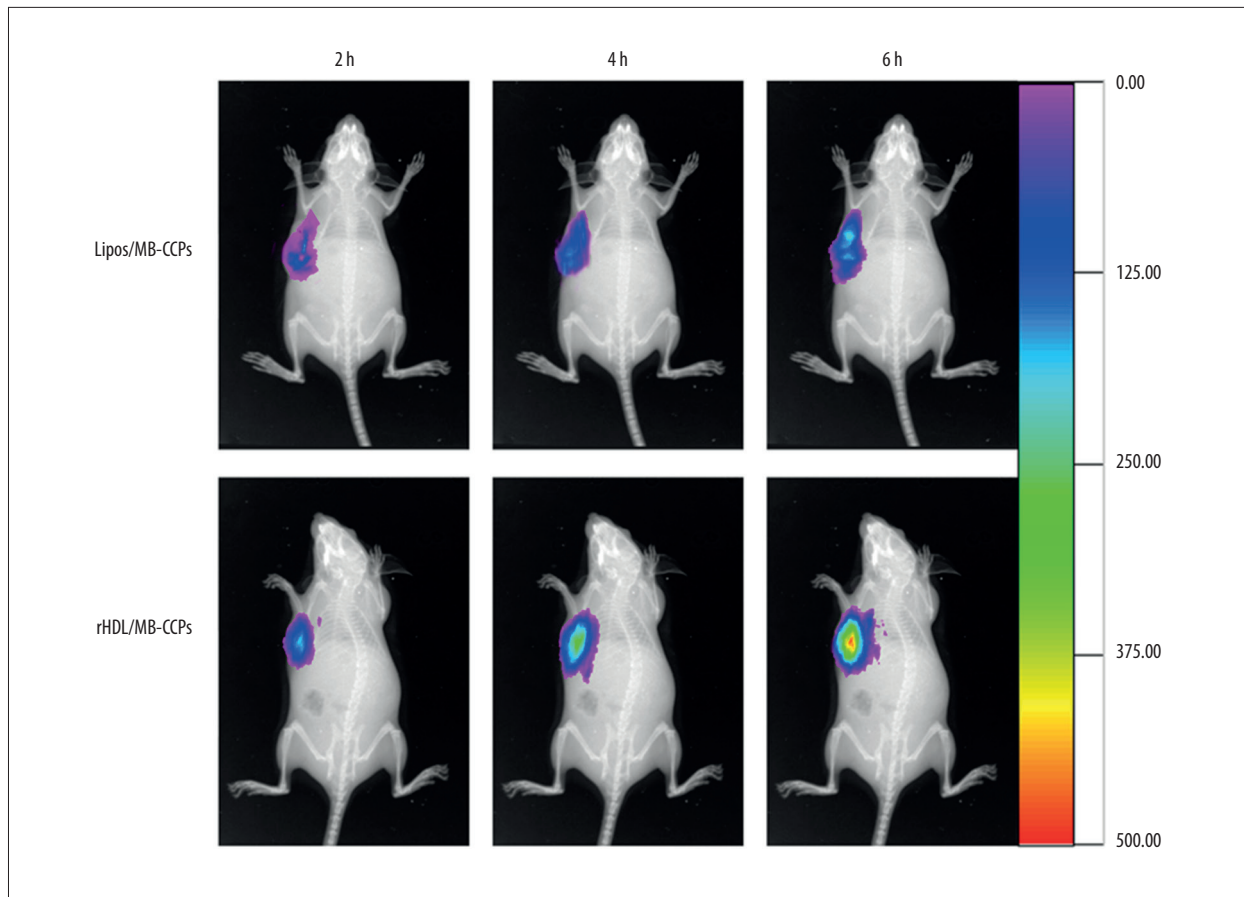


Figure 5. *In vivo* real-time imaging of Lipos/MB-CCPs and rHDL/MB-CCPs at various time intervals.

Discussion

The reverse water-in-oil micro-emulsion is composed of many nano-sized water pools which can provide space for diameter-controlled reaction. When the CCPs were formed, MB was incorporated into CCPs by absorption and/or embedment to formulate MB-CCPs. In the preparation of MB-CCPs, an amphiphilic phospholipid DOPA was added into the carbonate part of the reverse microemulsion. DOPA is known to strongly interact with cations, especially Ca^{2+} , at the interface [11]. It is expected that the MB-CCPs core should be coated with DOPA because excess Ca^{2+} should be available on the MB-CCPs surface. The alkyl chains of DOPA were sufficiently hydrophobic that the coated MB-CCPs were soluble in a non-polar solvent, which could be further modified by DOPC and cholesterol to construct a liposome (Lipos/MB-CCPs). The rHDL/MB-CCPs were eventually generated by the interaction between phospholipids of Lipos/MB-CCPs and apoA-I (Figure 6).

The particle size and zeta potential are in excellent relation to the performance of the delivery system and need to be carefully tuned to achieve the optimal therapeutic effect in cancer treatment. Multiple studies have demonstrated that

the biodistribution behavior and cellular uptake efficiency of nanoparticles are relevant to their particle size and zeta potential [12,13]. In general, smaller size usually leads to preferable cellular uptake and superior therapeutic effect of particles because they can be readily recognized and transported by the corresponding receptor or channel. On the other hand, it has been demonstrated that positively charged particles tend to interact with negatively charged serum proteins (such as albumin) and red blood cells after intravenous injection into the circulatory system, thus leading to preferable uptake by the reticuloendothelial system (RES) [14]. The rHDL/MB-CCPs showed nanoscale size of approximately 80 nm, with neutral surface charges, which might exert favorable biodistribution behavior *in vitro* and *in vivo*. Moreover, the core-shell structure indicated by the black arrows might be attributed to the apoA-I coating on the surface of rHDL/MB-CCPs, suggesting the successful anchoring of apoA-I on the surface of nanoparticles.

The use of a probe for cancer detection necessitates safety profiles, including BSA challenging, hemolysis, and cytotoxicity. In all, the results obtained from BSA challenging, hemolysis, and cytotoxicity assays provided decisive evidence that rHDL/MB-CCPs is a safe probe that can be used for *in vivo* applications.

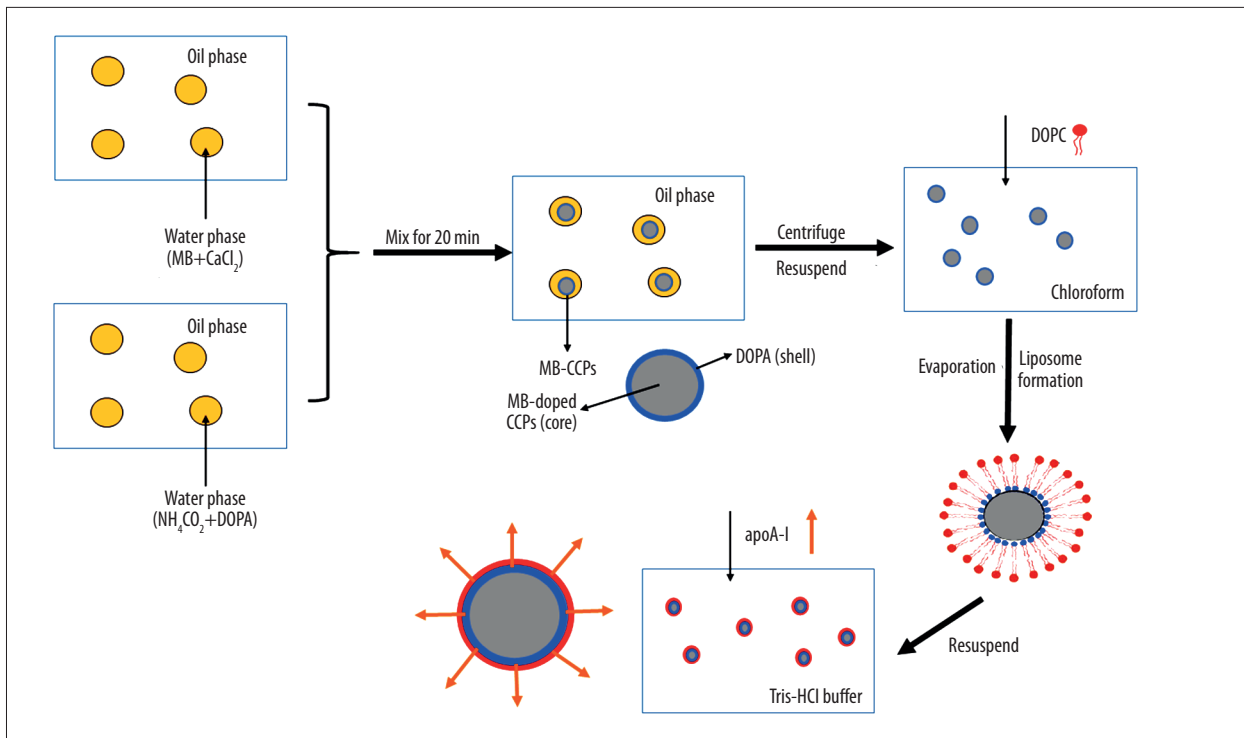


Figure 6. The formation process of rHDL/MB-CCPs.

MB, as an NIR dye, can emitted red fluorescence signals. The observed cytoplasm of A549 cells was all red, indicating that Lipos/MB-CCPs and rHDL/MB-CCPs successfully entered the cells. In addition, the fluorescence signal gradually became stronger with extended incubation time, indicating that the intracellular uptake of the nanoparticles increased in a time-dependent manner. The comparative fluorescence intensity between Lipos/MB-CCPs and rHDL/MB-CCPs suggested the superior cellular uptake profile of rHDL/MB-CCPs. To further elucidate the mechanism of rHDL/MB-CCPs internalization, a competitive experiment was performed by treating A549 cells with free apoA-I prior to incubation with the nanoparticles. As expected, fluorescence microscopy and flow cytometry demonstrated a decrease in the fluorescence intensity in tumor cells pretreated with apoA-I compared with the untreated cells. This result suggests that free apoA-I can competitively bind to SR-BI receptors and thereby block the binding of rHDL/MB-CCPs to these receptors, which confirmed that the nanoparticles predominantly entered into cells via a receptor-mediated pathway.

The *in vivo* biodistribution of rHDL/MB-CCPs in the A549 tumor-bearing nude mice model was determined with a non-invasive,

real-time, *in vivo* imaging technique to test the potential utility of rHDL/MB-CCPs as a probe in detecting A549 lung cancer. The superior tumor targetability of rHDL/MB-CCPs may be ascribed to the combination of EPR effect and SR-BI enhanced uptake mechanism. These findings provided decisive evidence that the designed rHDL/MB-CCPs were suitable as a tumor-specific probe for cancer detection.

Conclusions

In our study, a well-designed rHDL-based nano-system (rHDL/MB-CCPs) was successfully developed as a probe for cancer detection. The rHDL/MB-CCPs with diameter of approximately 80 nm and neutral surface charges demonstrated low protein absorption and hemolytic activity *in vitro*, with negligible cytotoxicity *in vitro* and *in vivo*. Above all, the rHDL/MB-CCPs exhibited SR-BI receptor-mediated cellular uptake behavior, which contributes to its specific tumor-targeting profile *in vivo*. In all, rHDL/MB-CCPs with high biocompatibility and targetability may serve as a promising probe for *in vivo* cancer detection.

References:

- Greenlee RT, Murray T, Bolden S, Wingo PA: Cancer statistics, 2000. *Cancer J Clin*, 2000; 50: 7–33
- Ballou B, Ernst LA, Waggoner AS: Fluorescence imaging of tumors *in vivo*. *Curr Med Chem*, 2005; 12: 795–805
- He X, Wang K, Cheng Z: *In vivo* near-infrared fluorescence imaging of cancer with nanoparticle-based probes. *Wiley Interdiscip Rev Nanomed Nanobiotechnol*, 2010; 2(4): 349–66

4. Deng T, Li JS, Jiang JH et al: Preparation of Near-Ir fluorescent nanoparticles for fluorescence-anisotropy-based immunoagglutination assay in whole blood. *Advanced Functional Materials*, 2006; 16: 2147–55
5. Ueno Y, Futagawa H, Takagi Y et al: Drug-incorporating calcium carbonate nanoparticles for a new delivery system. *J Control Release*, 2005; 103: 93–98
6. He X, Liu T, Chen Y et al: Calcium carbonate nanoparticle delivering vascular endothelial growth factor-C siRNA effectively inhibits lymphangiogenesis and growth of gastric cancer *in vivo*. *Cancer Gene Ther*, 2008; 15: 193–202
7. Shahzad MM, Mangala LS, Han HD et al: Targeted delivery of small interfering RNA using reconstituted high-density lipoprotein nanoparticles. *Neoplasia*, 2011; 13: 309–IN8
8. Vickers KC, Palmisano BT, Shoucri BM et al: MicroRNAs are transported in plasma and delivered to recipient cells by high-density lipoproteins. *Nat Cell Biol*, 2011; 13: 423–33
9. Li J, Yang Y, Huang L: Calcium phosphate nanoparticles with an asymmetric lipid bilayer coating for siRNA delivery to the tumor. *J Control Release*, 2012; 158: 108–14
10. Wang C, Bao X, Ding X et al: A multifunctional self-dissociative polyethyleneimine derivative coating polymer for enhancing the gene transfection efficiency of DNA/polyethyleneimine polyplexes *in vitro* and *in vivo*. *Polymer Chemistry*, 2015; 6: 780–96
11. Cotmore JM, Nichols G, Wuthier RE: Phospholipid – calcium phosphate complex: enhanced calcium migration in the presence of phosphate. *Science*, 1971; 172: 1339–41
12. He C, Hu Y, Yin L et al: Effects of particle size and surface charge on cellular uptake and biodistribution of polymeric nanoparticles. *Biomaterials*, 2010; 31: 3657–66
13. Limbach LK, Li Y, Grass RN et al: Oxide nanoparticle uptake in human lung fibroblasts: effects of particle size, agglomeration, and diffusion at low concentrations. *Environ Sci Technol*, 2005; 39: 9370–76
14. Wang C, Li M, Yang T et al: A self-assembled system for tumor-targeted co-delivery of drug and gene. *Mater Sci Eng C Mater Biol Appl*, 2015; 56: 280–85